Modern Ray-Based Modelling and Simulated Depth Migration for Survey Planning and Interpretation: A 3D VSP Example

Lars Zühlsdorff* and Håvar Gjøystdal**

**Åsmund Drottning, NORSAR Innovation AS, Norway*

***sabelle Lecomte, Stein Inge Moen, Håkan Bolin, NORSAR, Norway*

Abstract

For designing seismic surveys that fit the purpose, advanced seismic modelling is usually unavoidable. In the presence of complex geological structures, finite-difference modelling followed by data processing and imaging is a common and sometimes necessary approach. However, ray-based methods are by far more flexible and efficient, and they provide more than adequate results in most cases. This study focuses on some modern ray-based approaches that are routinely used for finding required survey parameters, for supporting seismic data processing and interpretation, and for simulating the best possible depth migration results, along with a direct measure of achievable lateral and vertical resolution. Among a summary of existing methods, two new techniques are introduced: (1) a target-point oriented fast-track approach that provides an overview over required key survey parameters even before a full survey configuration is designed, modelled and analysed, and (2) an updated ray-based method for simulating pre-stack depth migration images that is valid on a reservoir scale.

Introduction

Using appropriate subsurface models and finite-difference (FD) modelling, full wavefield synthetic data can be generated and subsequently migrated in order to simulate the final outcome of specific survey geometries. This is especially useful if the efficiency of processing workflows to suppress noise or multiple reflections needs to be tested (e.g., Houbiers et al., 2008; Stork, 2012). However, both FD modelling and imaging may still be expensive with regard to computer time and memory. Consequently, modelling and processing parameters cannot be varied easily to carry out efficient sensitivity studies, and the frequency bandwidth of modelled results is often limited to reduce computational effort.

Ray-tracing is done in smooth macro-models and is a comparatively fast and flexible approach (Gjøystdal et al., 2007). Rather than modelling the full wavefield, ray-tracing is a target oriented process that can be used to study primary or multiple reflections from specific interfaces. A key advantage of ray tracing is that reflection points are known, and thus the generation of illumination maps is possible. For many years, ray-based illumination studies have been used by the industry as a basis for survey planning (e.g., Bear at al., 2000; Ibrahim, 2005). Today, survey planning may be considered as most complete if the advantages of both FD modelling and ray-tracing are successfully combined, e.g., if ray-tracing is used to plan for a final FD run or to identify primary and multiple reflections in both FD-modelled and field seismic data (e.g., Christian et al., 2012).

Even though the wealth of FD modelling is undisputed, results can be as difficult to interpret as field records and may therefore require ray-based support. Also, many survey design studies can be completed successfully by using ray-based methods only. This is because such methods have developed a lot since the early days of two-point ray-tracing, as also discussed by Gjøystdal et al. (2007):

- Wavefront construction (Vinje et al., 1999) allows for adaptive control of ray density throughout the model and for modelling huge source and receiver geometries in comparatively short time.
- 3D ray-tracing models can be very complex (including overhang structures, truncations, open and closed salt volumes, gas-filled zones and undefined areas). They can also be anisotropic (i.e., transversely isotropic with vertical or tilted axis of symmetry).
- Mode conversions, multi-pathing (i.e., more than one recorded event for each given shot and receiver pair), and complex ray-paths (including primaries, intra-bed multiples, ghosts, and rays related or not related to specific subsurface features) can be taken into account.
- Depth migration amplitudes can be simulated and mapped on the fly by migrating specular ray-tracing events along target interfaces and within the first Fresnel zone (Laurain et al., 2004).
- Source modelling (usually for marine gun arrays) can be combined with ray-tracing to take source directivity and appropriate far-field wavelets into account when generating synthetic seismograms.
- Kirchhoff modelling (e.g., Frazer and Sen, 1985; Tygel et al., 1994) utilizing ray-based algorithms to obtain Green's function attributes can be used to simulate edge diffractions and to provide realistic synthetic seismograms that can be migrated without generating unnecessary artefacts.
- Illumination rays can be used for finding potential shot and receiver combinations that illuminate a specified target point. Results are given as rose diagrams in either azimuth offset domain (survey related) or incident-

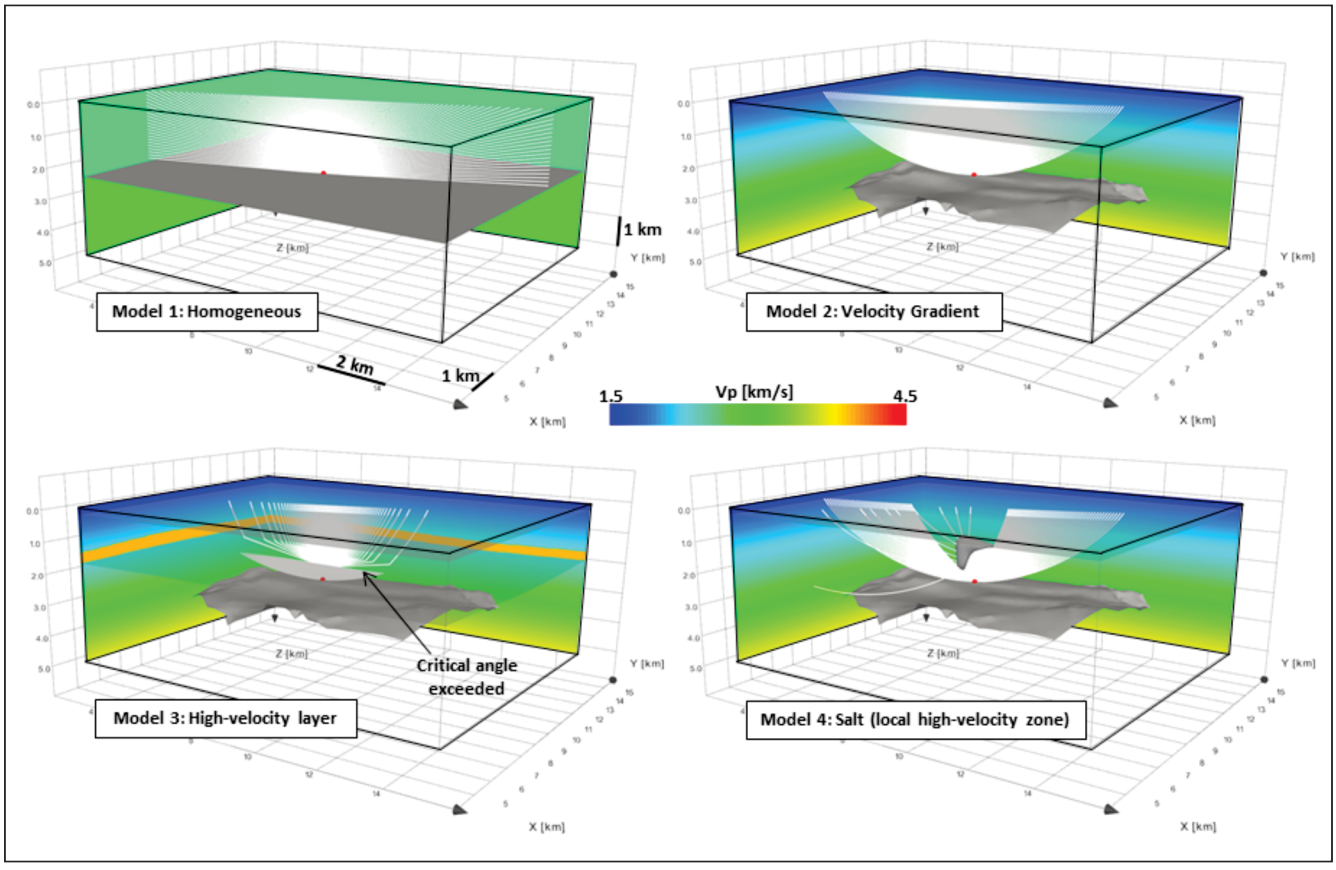

Fig. 1 : Different model versions for testing the effect of velocity field variations and target topography. Model 1: A homogeneous overburden above a horizontal target. Model 2: A vertical velocity gradient above a more realistic target. Model 3: An additional high velocity layer. Model 4: A local high velocity zone (salt) rather than a high-velocity layer. Rays shown here (for a selected target point and azimuth) are independent of any survey and indicate general ray behavior within each model.

azimuth incident-angle domain (target related). This is a rather new technology, which is summarised below as part of this study.

- Illumination vectors, which are valid for representative scattering points in the sub-surface, can be utilized to simulate pre-stack depth migration (PSDM) images of selected target volumes directly from a model (e.g., Lecomte, 2008; Drottning et al., 2009). The associated point-spread functions (PSF) provide a direct measure of both lateral and vertical resolution. It is demonstrated below how larger target volumes or even full reservoirs can be imaged by combining variable PSFs and assembling the associated sub-volumes to a final cube or image.

Motivation

The model used in this study is purely synthetic. The overburden can be easily modified to test the effect of different velocity fields or the impact of additional subsurface features like salt bodies (Figure 1). Thus, this is not a case study but an introduction to ray-based modelling and survey planning concepts. These concepts are of general nature and not necessarily related to any specific survey geometry, i.e., all examples as generated below could be easily adapted to various types of marine or land surveys. However, a three-dimensional setup for vertical seismic profiling (3D VSP) was chosen because of its unconventional survey geometry and limited aperture, which formerly was a challenge for simulating pre-stack depth migration images. Also, VSP can be done onshore as well as offshore and thus does not imply any specific environment.

Ray-based approaches and 3D VSP Examples

A common goal of any survey design study is to find the minimum required survey geometry, i.e., appropriate shot and receiver locations, offsets and azimuths to illuminate the target area of interest, to provide sufficient fold, to cover sufficient incident angle and incident azimuth ranges, and to allow for sufficient resolution. However, it makes sense to start with some more general survey parameters, in order to gain some understanding of the required type, size, location and rotation of the shot and receiver setup.

Defining key survey parameters

Key survey parameters are usually determined from illumination studies. Criteria for selecting a survey setup for further consideration could be the number of reflection points inside the target area, the range of incident angles, acquisition footprint, estimated amplitudes, expected migration aperture, required recording time, or any other parameter that can be a direct result of advanced ray-based modelling.

However, as survey geometries are input to seismic modelling (and not only the final result), it is usually required to model and compare different shot and receiver configurations in order to define the most successful option. Using ray-tracing, there are several ways for doing this very efficiently:

(1) Survey decimation: As the mathematical foundation of ray-tracing is based on a high-frequency approximation of the wave equations, ray-tracing needs to be done in sufficiently smooth macro-models. This usually is no disadvantage for any application in the fields of seismology and exploration seismics. However, on lateral scales of 10 -100 m (i.e., the range of typical shot spacing), modelling results will not be much different. Rather than modelling a survey in full, it may therefore be sufficient to model only every second or third shot, reducing processing time to 50% or less. Illumination maps can then be easily calibrated to simulate a result for all the shots.

(2) Analytical surveys: It may make sense to use rather large shot and receiver grids for modelling, i.e., a geometry that would never be used in the field but contains a number of different survey options. If set up correctly, more than one task can be carried out within a single modelling run. Respective results can then be extracted by appropriate shot or receiver sub-selections, automatic splitting of parameter sets into offset or incident-angle ranges, filtering on specific event attributes, or switching between different mapping domains (some examples are given below).

(3) Coarse patch modelling: In many cases, coarse shot grids in combination with sufficiently large receiver grids, which may or may not be following the shots, will provide a fast-track preview of full-survey results. If set up correctly, sensitivity of illumination attributes to survey azimuth or offset can be tested on a single set of modelled events.

(4) The concept of reciprocity: If only P-waves are modelled, shots and receiver positions can be flipped without affecting final illumination maps. This is an option if there are many more shots than receivers, e.g., in case of 3D VSP surveys with limited numbers of receivers along the well track. If ray-tracing is done by wavefront construction, modelling time will decrease almost linearly with a decreasing number of shots.

These concepts are rather general and may be of use when planning any type of seismic survey, including 3D VSP. VSP implies that receivers are located along a well track and shots are located at the surface. Such surveys often do a good job in illuminating seismic targets at high resolution and close to a well, especially if surface seismic is suffering from near-surface effects in the overburden. Typical 3D VSP shot patterns include multiple walkaway shot lines in different azimuths from the well, a regular grid of shots, or a spiral of shots centred on the well.

Key 3D VSP survey parameters include maximum offset (the distance of shots to the well head) and imaging radius (the size of the target area around the well that can be imaged). In principle, the imaging radius can be easily increased by increasing the offset, but there is a natural limitation, as rays may never reach the target due to critical angles in the subsurface, or as ray-paths may become very complex and thus are difficult to utilize for imaging (e.g., Lou et al., 2011).

There is no obvious physical criterion for defining the maximum imaging radius, and using a straight-line approximation (i.e., assuming homogeneous overburden above a horizontal target) often over-estimates the size of the area that can successfully be imaged (Lou et al., 2011). However, limiting 3D VSP travel-time for a specific target to the zero-offset two-way travel-time for a shot and receiver location right at the well head is a reasonable approach (adapted from Lou et al., 2011). This is because VSP reflection signals with longer travel-time most likely are associated with complex ray-paths and are not any longer expected to have wider frequency bandwidth than the corresponding surface data. Such a travel-time limitation can be easily utilized during an illumination study by applying an appropriate attribute filter.

For the following example, shots were located along a spiral with 50-m shot spacing and 200-m spacing between the spiral's arms. Maximum offset was set to 5 km, which was considered to be “sufficiently large” and was supposed to be optimized as a result of the illumination study. Receivers at 15-m spacing were located all along a vertical well above a target at 2.4 km depth. As there were many more shots than receivers, shot and receiver positions were flipped and a single modelling run on the full (analytical) survey was done in just a few minutes (on a small 20-node Linux cluster).

Distributing receivers all along the well for modelling allows for testing the impact of different receiver depth ranges on illumination attributes by using appropriate receiver sub-selections during map generation. Images shown here were generated for receivers at 1000-2000 m depth. Figure 2 shows the survey setup and the number of hits in each bin cell for a homogeneous reference model and a flat target interface (Model 1). Using such a model, a straight-line equation for calculating the imaging radius is fully accurate if no other criterion (e.g., a travel-time limitation) is used.

In the field, the situation is typically much more difficult, as targets are not necessarily flat and the overburden is never completely homogeneous. Thus, a straight-line equation can only provide an approximation of the imaging radius. Figure 3 shows the same kind of hit map as in the previous image, but the homogeneous overburden model was now replaced by a velocity gradient and also some target topography was introduced (Model 2). This model is still rather simple, and the straight-line approximation for the imaging radius is reasonably good, even though the rays are slightly bending and the hit pattern differs significantly from the reference case. However, the modelled imaging radius is much smaller than the straight-line approximation if a travel-time limitation is introduced (2.4 s, which is the two-way travel-time for a zero-offset receiver at the surface). Depending on

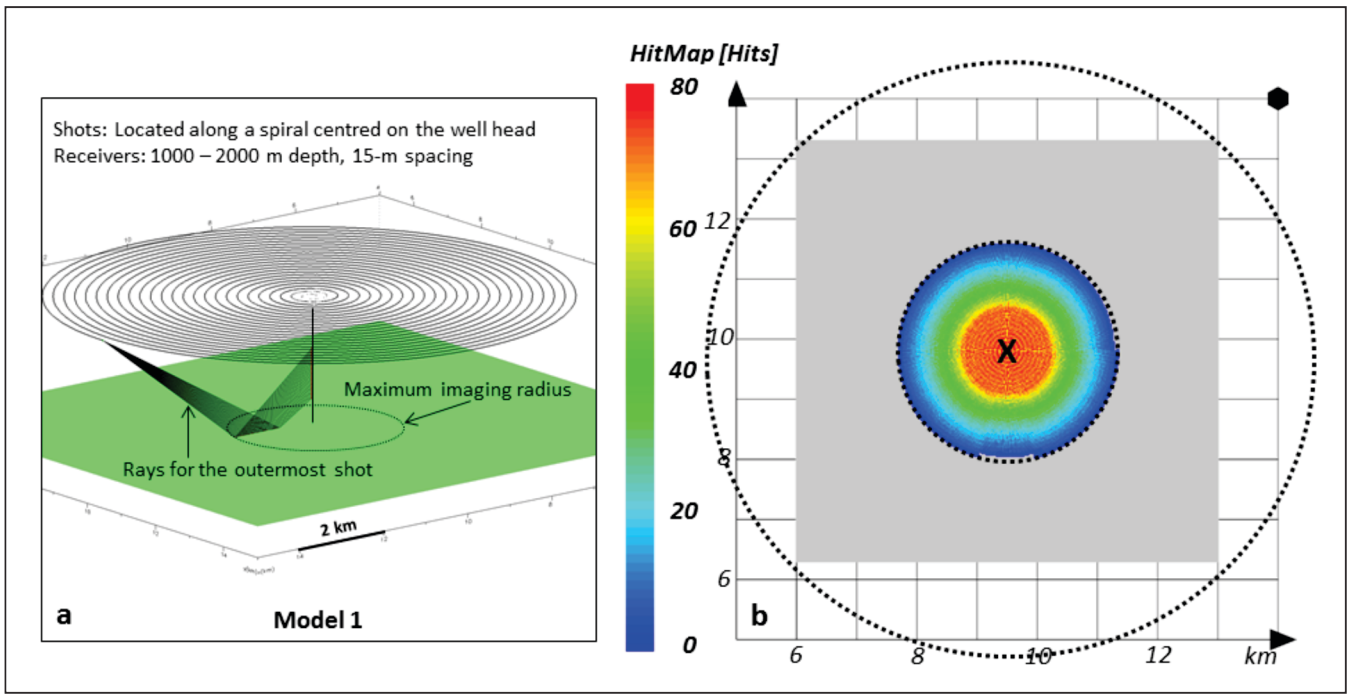

Fig. 2: (a) Survey setup. (b) Reference map showing the number of hits within each bin cell (25 m x 25 m) for a homogeneous overburden model and a flat target (Model 1). The cross at the center marks the well position, and the inner circle indicates the imaging radius as based on a straight-line equation. The larger circle outlines the shot area.

the overburden, a straight-line approximation tends to over-estimate the imaging radius and can therefore be misleading.

Rather than generating maps in the target-domain to determine the imaging radius, maps can also be generated in the shot-domain to determine the maximum usable offset (Figure 4). The same travel-time limitation as before is used, and the colour scale range is limited accordingly as the attribute to be mapped now is minimum travel-time. Thus, red colours indicate shots that generate events with equal or larger travel-time than the two-way travel-time for a zero-offset receiver at the surface. All colours, which are not red, therefore indicate usable shots for the 3D VSP survey. Note that the usable shot area is not necessarily centred on the well head. This is demonstrated by introducing a slightly tilted high velocity zone to the overburden, which also slightly increases the usable maximum offset (Figure 4) but not necessarily the imaging radius (see rays in Figure 1 for illustration).

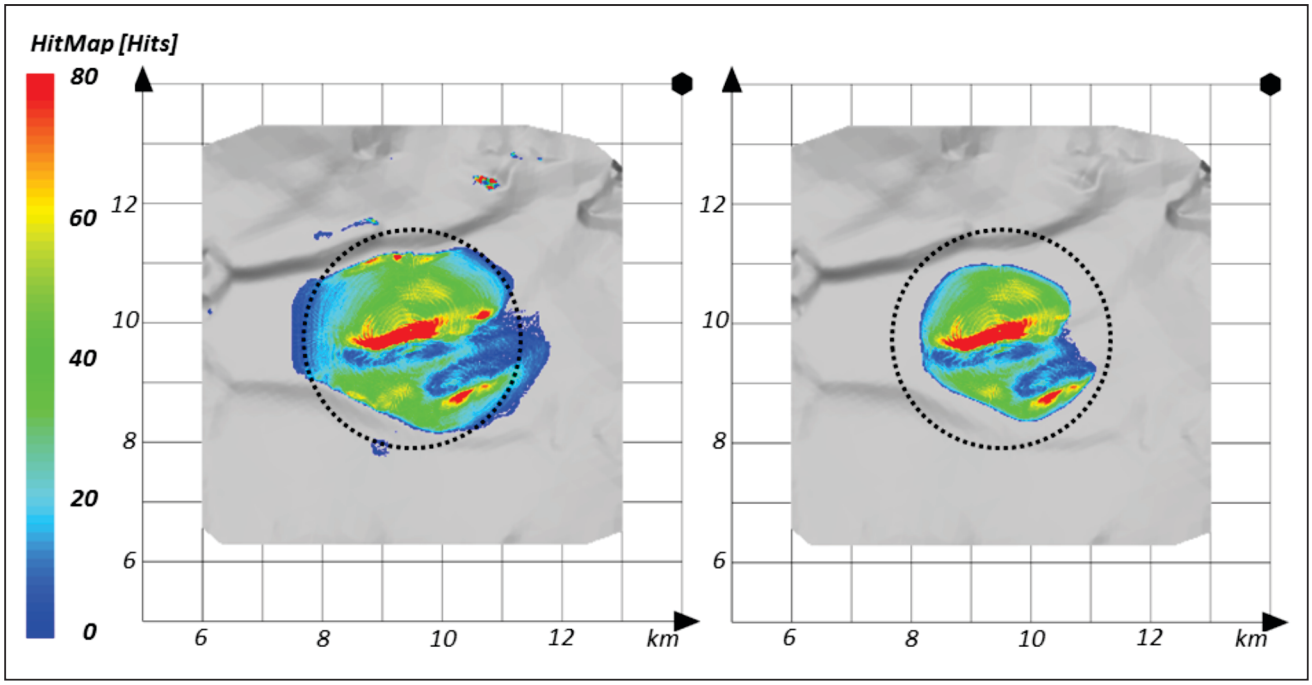

Fig. 3 : Same type of map as in the previous figure, but for Model 2 rather than for Model 1. The straight line approximation for estimating the imaging radius is indicated by the circles. Left: Using all modeled events, i.e. a maximum offset of 5 km. Right: Using a travel-time limitation.

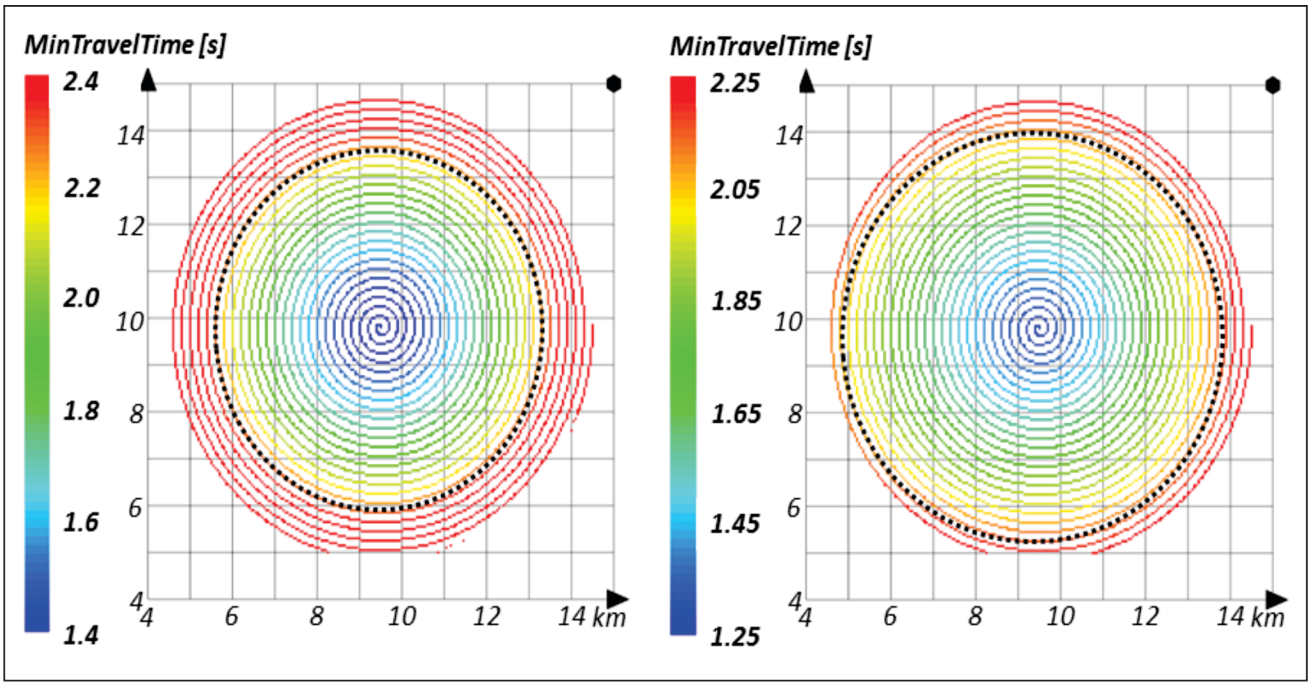

Fig. 4 : Shot-domain maps indicating the usable shot area (circles) for two different models. Left: A velocity gradient above the target (Model 2). Right: An additional and slightly tilted high velocity zone in the overburden (Model 3). The color scale is limited to the two-way travel-time for a zero-offset receiver at the surface, which is different for the two models.

Similar concepts are used for comparing requirements for salt-flank illumination and salt proximity testing. Salt-flank illumination requires rays that are reflected at the salt-flank, whereas a salt proximity test would make use of rays transmitting the salt. Again, an analytical survey is used for the modelling, i.e., a much larger shot grid is defined than would be used in the field. However, receivers are limited to the lower most 500-m depth interval of the well in order to generate the maps in Figure 5 (as testing indicated that salt-flank coverage is very limited for shallower receivers).

Hit count maps were generated in both target- and shot-domains. Target-domain maps indicate where reflection or transmission points are located on the salt-flank. In the given case, a larger area on the salt-flank is covered if transmission points rather than reflection points are utilized. Shot-domain maps indicate the location of shots that contribute most to target reflection or target transmission. In the given case, the area that confines the most efficient shots is smaller and much closer to the well if the salt is to be transmitted (Figure 5).

Interpretation support

It is important to take practical aspects into account when analysing ray-tracing results. Illumination maps that show complete and sufficient coverage can be misleading if the

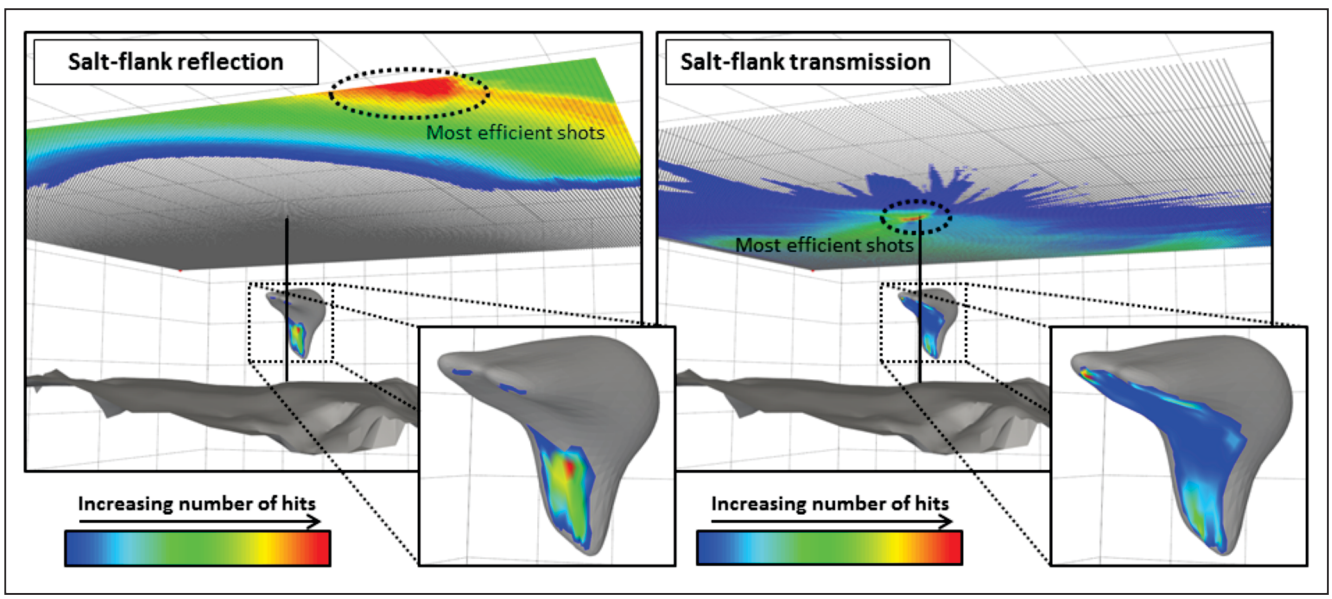

Fig. 5 : Combination of shot domain and target domain maps for salt flank illumination (left) and salt proximity testing (right).

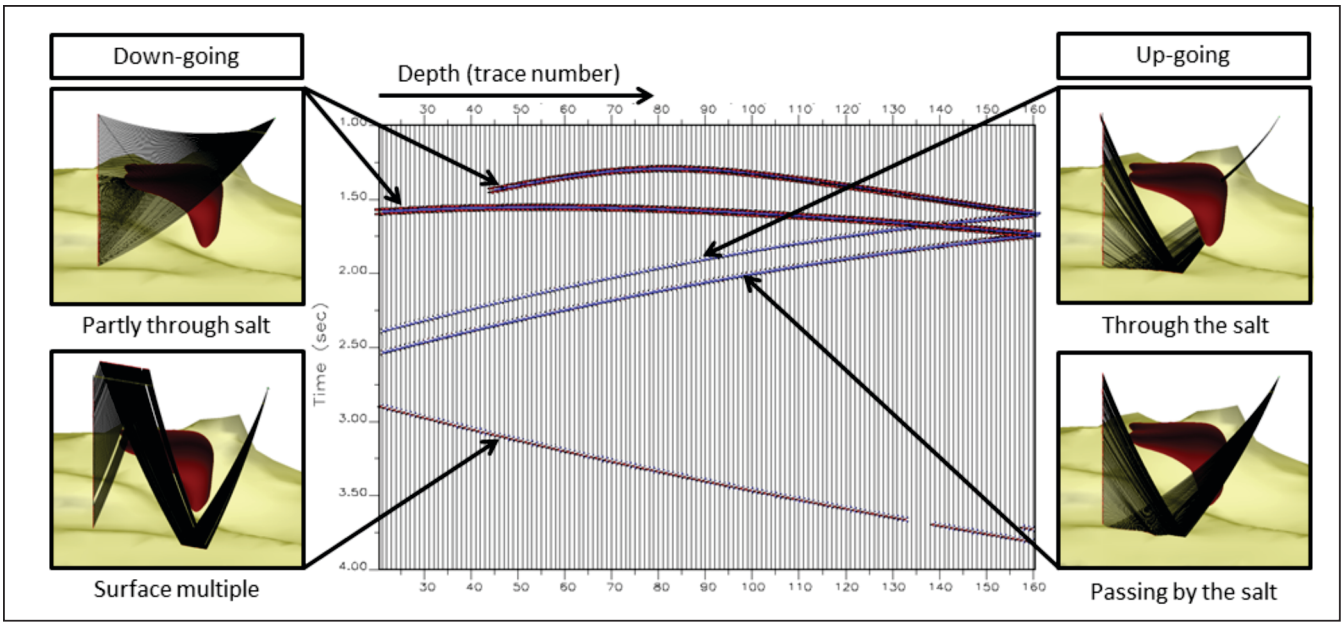

Fig. 6 : Different parts of the wavefield as modeled by ray-tracing. The model above the target consists of a velocity gradient and a salt volume (Model 4).

associated ray-paths are too complex for migration, migration apertures are too large, multiple events cannot be utilized or multiples cannot be distinguished from primary reflections. FD modelling and subsequent data processing clearly is an option to test migration and de-multiple algorithms beforehand.

However, another advantage of ray tracing is that only specified parts of the wavefield are modelled, and that these parts can subsequently be identified in both field data and FD modelling results. Ray-tracing and FD modelling therefore can be considered as complimentary methods. Ray-tracing can also distinguish between recorded events for different ray-paths between the same shots and receivers and may thus help to identify areas that suffer from complex ray behaviour. In the special case of VSP geometries, it may be useful to model down-going and up-going wavefield separately (Figure 6).

Target-point related analysis

Ray-tracing typically is shot-related rather than target-point related. The reason is that surveys are recorded as shot gathers, and thus many shot gathers need to be combined and sorted in order to collect complete information about specific target points. As the required shot and receiver positions are not known beforehand, this can be a challenging and time consuming task, especially if many different target points need to be considered.

However, target point related information can be generated by constructing illumination rays, i.e., rays that connect shot and receiver positions at the surface and reflect at the selected target point obeying Snell's law (specular reflection). If this is done efficiently, target point related analysis can even be done interactively, e.g., by keeping the incident azimuth constant and displaying rays for all

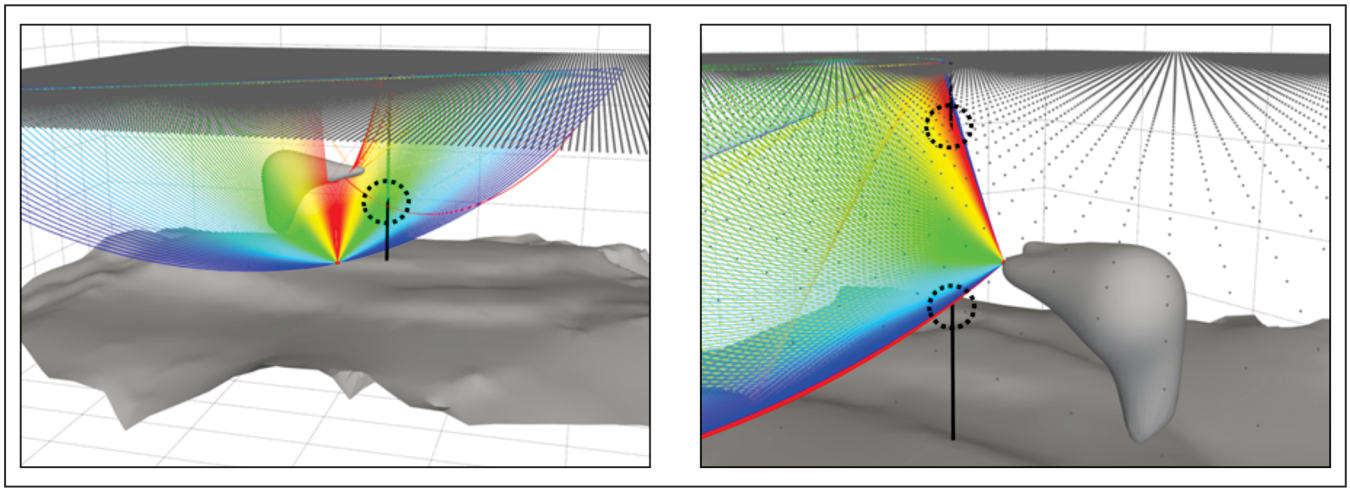

Fig. 7: Interactive illumination ray generation in fan mode (left) and cone mode (right). Circles indicate where the fan/cone intersects the well track. The coloring has no specific meaning but changes with incident angle or incident azimuth to guide interpretation.

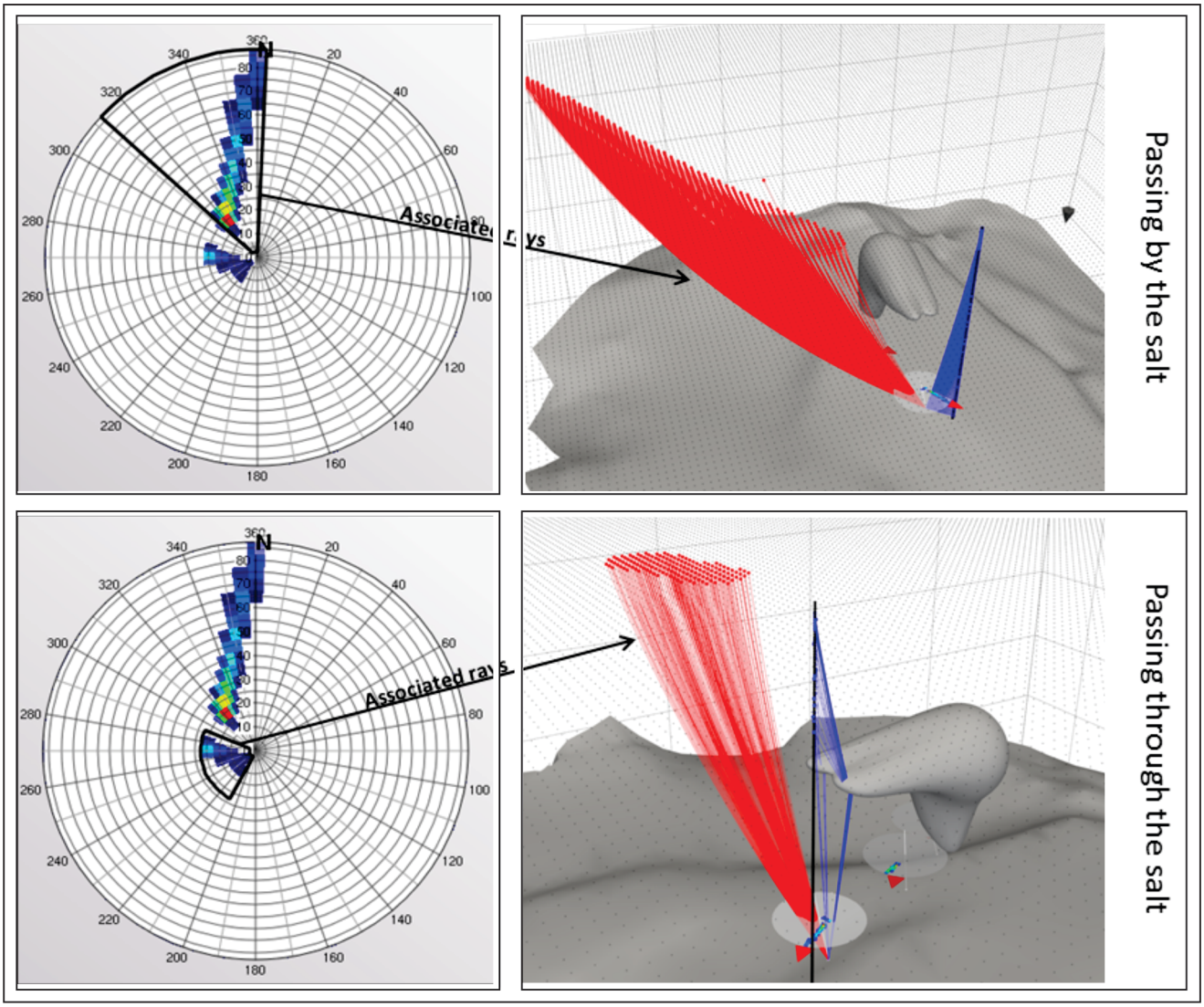

Fig. 8: Target-related rose-diagrams (i.e., the circular scale indicates incident azimuth, whereas the radial scale indicates incident angle). Events in marked cells were re-traced to indicate shot locations (at the surface) and receiver locations (in the well). Thus, red rays are down-going and blue rays are up-going.

incident angles (fan mode), or by keeping incident angle constant and displaying rays for all incident azimuths (cone mode). This provides quick understanding of general ray behavior at different target areas of interest and some important relationship between angles at target level and survey properties at surface level. In case of a 3D VSP geometry, the intersection of the respective fan or cone with the well track provides information about the required offsets between the associated shots and the well head (Figure 7).

Analyzing all incident angles and all azimuths for a single target point or a range of target points requires generation of rose-diagrams. These can either be target related (incident azimuth incident angle domain) or survey related (azimuth offset domain). In both domains, shots or receivers can be freely distributed at the surface or confined to any given survey geometry. In case of VSP, it should be taken into account that receivers are only distributed along a well track. Final rose diagrams provide detailed information about expected incident angle ranges as well as offset and azimuth requirements for potential surveys. As illumination rays are explicitly generated for a specific point of interest, it is easy to retrace rays that belong to a specific cell or a group of cells in rose diagrams and relate these to the respective shot and receiver positions (Figure 8). Thus, key survey parameters can be determined even before any full illumination study is carried out and the required full-scale modelling can be planned more thoroughly and more efficiently.

Imaging and resolution

Simulating depth migrated images can be a quick process, if the approach is based on fast-Fourier transformation (Lecomte 2008). Results are still consistent with the given survey, wavelet, overburden and reservoir properties. In order to achieve that, illumination vectors can be generated for any selected sub-surface scattering point. This is a result of ray-tracing in a smooth overburden model

and fully independent of any reservoir interface to be imaged. Each illumination vector carries, e.g., information about the dip that can be illuminated by the respective shot and receiver combination. The full set of illumination vectors as based on all possible shot and receiver pairs therefore carries information about all dips (and azimuths) that can be illuminated by the full survey and the given overburden model.

Illumination vectors are then converted into scattering wavenumber vectors and thus into a wavenumber filter (called PSDM filter in the following), which may also incorporate the features of a given wavelet (Lecomte, 2008). Finally, this PSDM filter can be applied to any reservoir model, which is defined in terms incident-angle dependent reflectivity and was previously transformed into the wavenumber domain. Dips that pass the PSDM filter are kept for imaging as the migrated image in depth-domain is obtained by inverse Fourier transformation.

Typically, a single PSDM filter is used as based on a single scattering point in the sub-surface. In such a case, the simulation is only valid within a representative volume around the scattering point. Accordingly, the filter can only be applied to a sufficiently small portion of the reservoir. This is fine for surface seismic data, as the representative imaging volumes can still be rather large (e.g., Zühlsdorff *et al*., 2010).

However, if overburden models include rapid lateral velocity changes (e.g., salt domes) or if survey geometries with limited aperture are used (as for 3D VSP), the representative imaging volumes can become very small. In such cases, spatially varying PSDM filters need to be combined within the same workflow in order to generate correct images. In

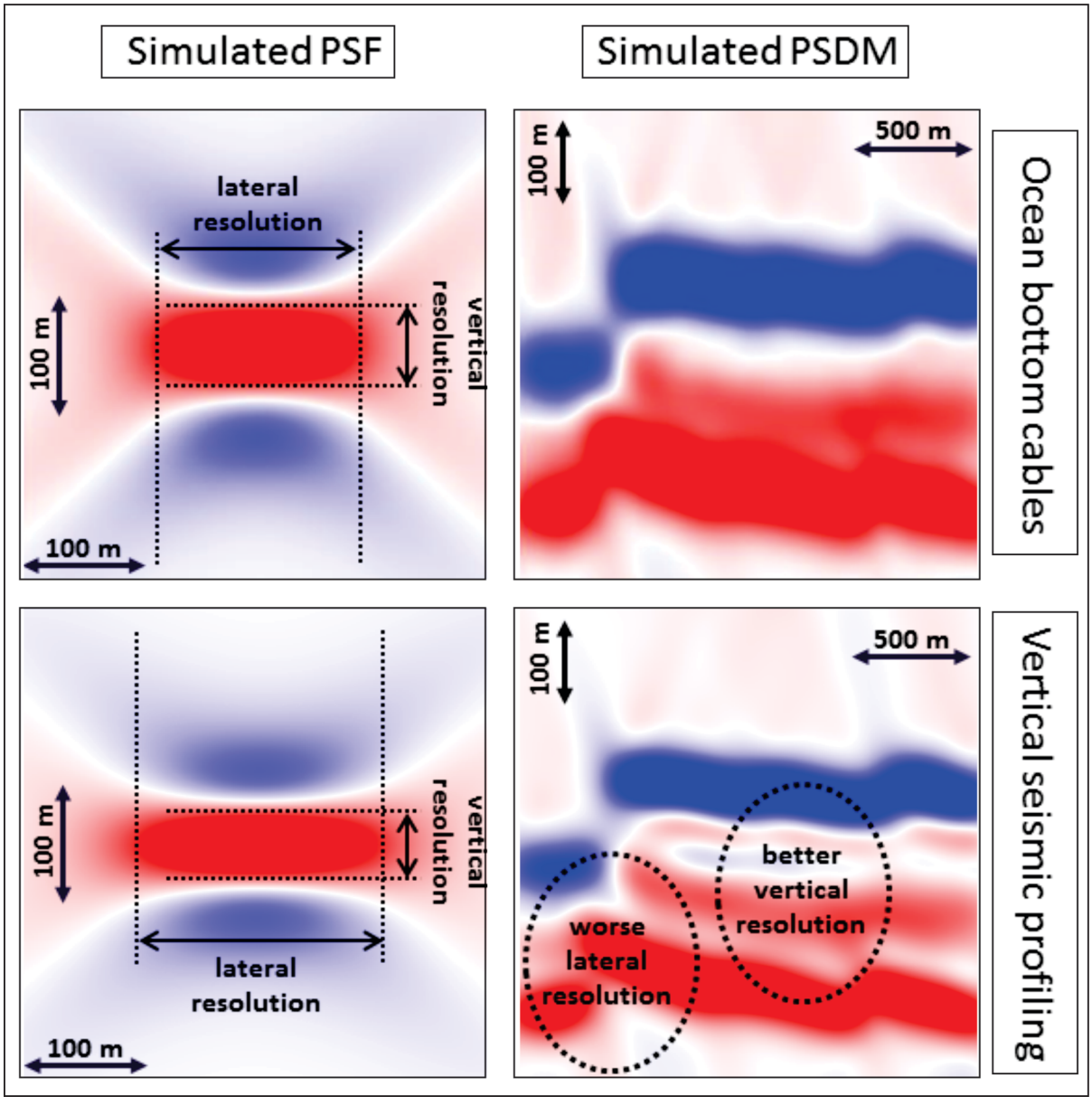

Fig. 9: Point spread function (PSF) and simulated pre-stack depth migration (PSDM) for an ocean bottom cable survey (top row) and a 3D VSP geometry (bottom row). Note the differences in both vertical and lateral resolution. Results were generated for Model 2.

other words, spatial variation of illumination and resolution cannot be represented by a single (local) PSDM filter but requires an appropriate distribution of such filters.

To illustrate this, pre-stack depth migration was first simulated for a 3D VSP setup (500-2000 m receiver depth) and an ocean bottom cable (OBC) geometry, using the same 50-Hz input wavelet for the computation. Both survey configurations were made comparable with regard to the illuminated target area. Only a single PSDM filter inside the reservoir was generated, and it was assumed that zero-offset reflectivity is valid for all incident angles. Results were compensated for geometrical spreading but not for intrinsic attenuation. However, as the reservoir is only a few hundred meters thick and located at >2.4 km depth, only slight intrinsic attenuation was introduced to the model (Q=1000).

Simulated depth migration images and their related PSFs are compared in Figure 9. A PSF (in depth-domain) is the inverse Fourier transform of a PSDM filter (in wavenumber-domain). As such, the filter could also be applied in depth domain by convolving the given PSFs with the input reflectivity cube. PSFs therefore indicate how far a single point is spatially spread after passing the filter and thus provide a direct measure of both vertical and lateral resolution.

The achievable vertical resolution is better for 3D VSP, which is expected due to the shorter ray-path and the lesser effect of intrinsic attenuation. However, lateral resolution is better for OBC. This is because the larger receiver aperture of the OBC setup is directly related to a larger aperture of the corresponding PSDM filter in wavenumber-domain (and thus to a sharper PSF in lateral direction). This effect is similar to the Fourier-transform relation between time-domain and frequency-domain in signal processing: wider bandwidth in frequency domain corresponds to a shorter signal in time domain and thus to better temporal resolution (see results and discussion in Lecomte, 2008). With regard to spatial resolution, PSFs incorporate the effect of both attenuation and survey geometry and thus provide a practical aid to evaluate seismic surveys.

This, however, is only part of the story, as the reflection coefficient is angle-dependent and results need to be decomposed into different incident-angle ranges for a fair comparison (Figure 10). Results for 3D VSP turn out to be very angle dependent, which again is due to the receiver distribution along the well. As the filter was generated for a single scattering point right beneath the receiver string in the well, contributions from small incident angle reflections are expected to dominate the image (but some other events contribute as well, as there is target topography and a velocity gradient in the overburden). However, the further away from the well a target point is located, the larger are the required offsets and thus the required incident angles to illuminate that point. As such, a single PSDM filter is not sufficient to simulate pre-stack depth migration for 3D VSP.

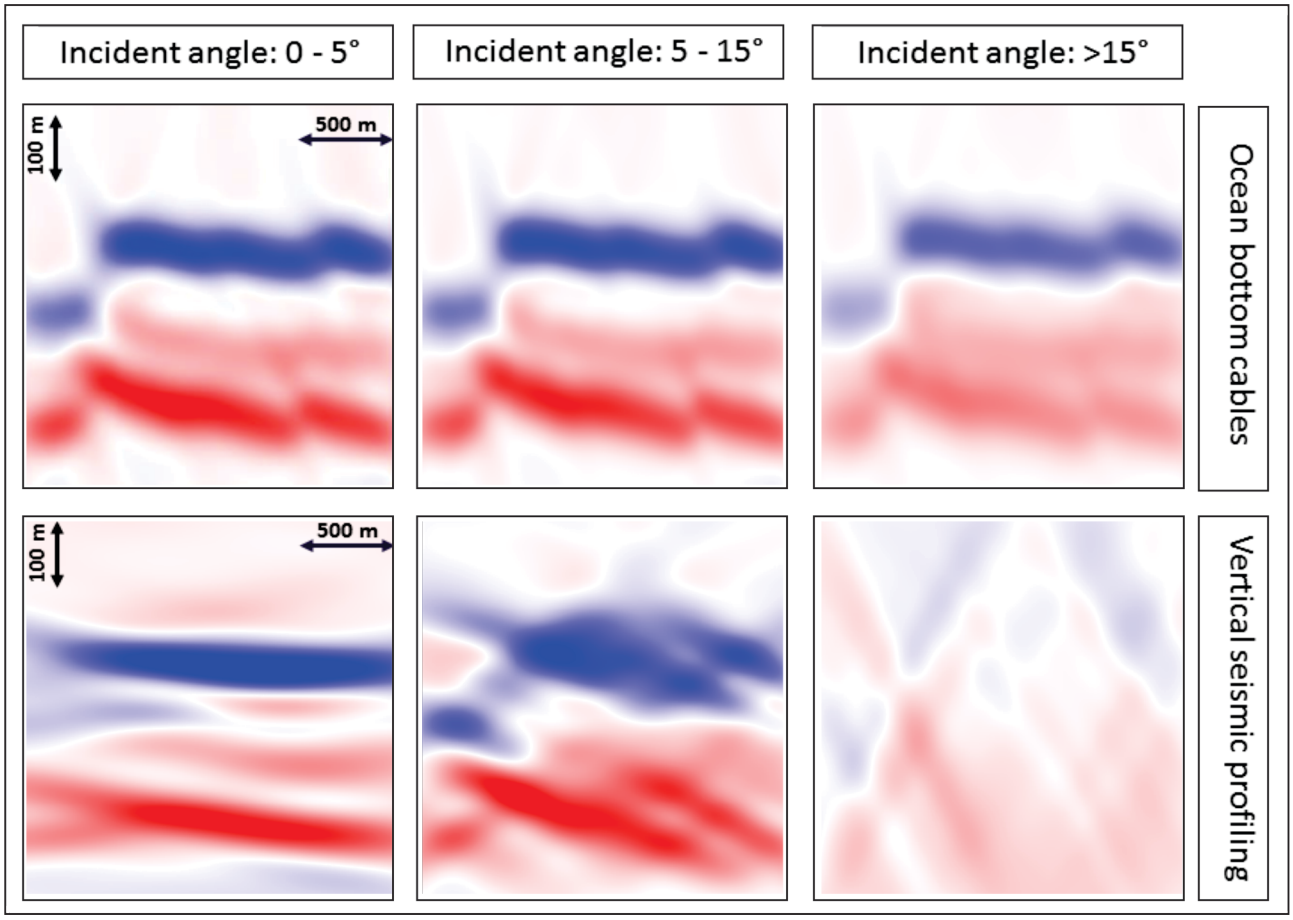

Fig. 10 : The same PSDM results as shown in the previous figure, but decomposed into different incident angle ranges.

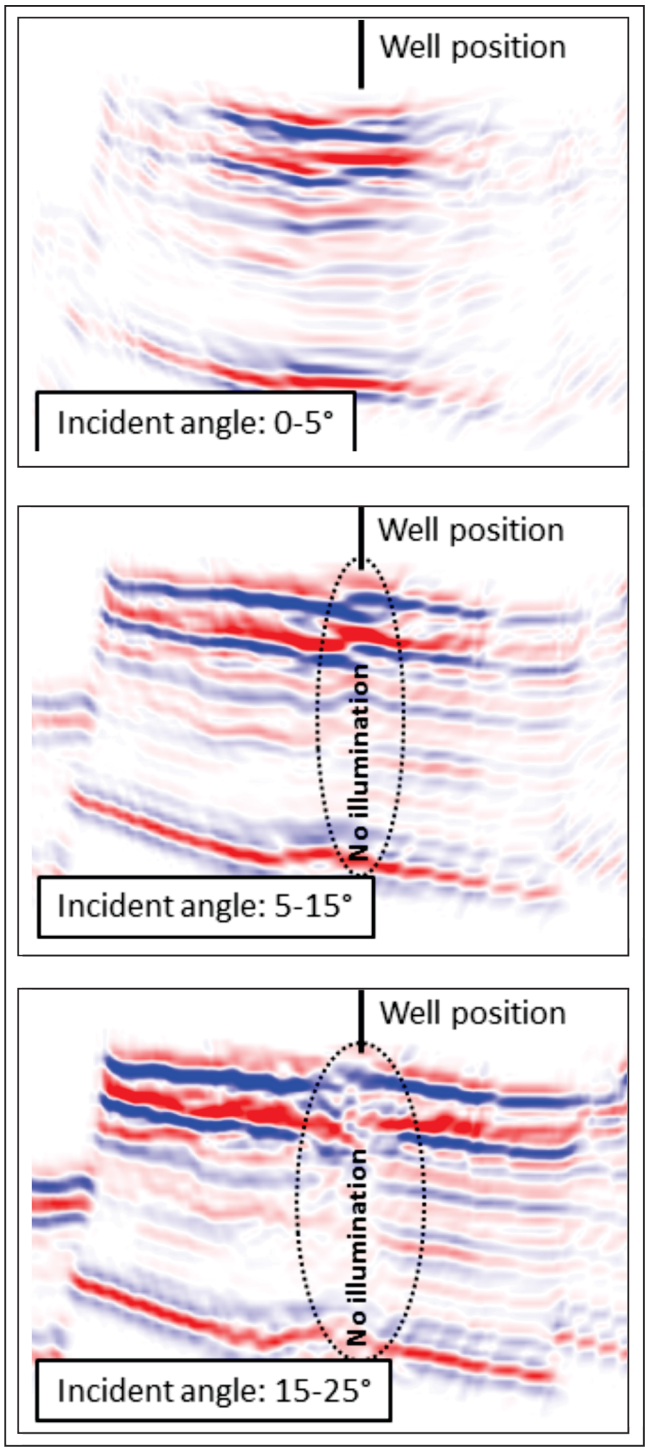

Fig. 11 : Simulated depth migration images of the reservoir around the well. Each line is 1.4 km long and the respective boxes are 400 m high. Results were generated for Model 2. For larger incident angles there is no illumination close to the well, but the blank zone is obscured by energy smearing in from the sides due to the effect of limited lateral resolution.

Consequently, a grid of 13 x 13 variable filters at 200 m spacing was used to re-model the 3D VSP case. The scattering point the central PSDM filter is based on is still located beneath the well. Each PSDM filter generates depth migrated data within a 200 x 200 x 600 m volume, and all 169 sub-cubes are assembled to a single cube that contains a larger portion of the reservoir (2.4 x 2.4 x 0.6 km, a slightly smaller portion is shown in Figure 11). Intrinsic attenuation was neglected in this case, in order to provide higher resolution images. A travel-time limitation of 2.4 s was applied (as this is the two-way zero-offset travel-time for Model 2 and the given target).

Again, the 3D VSP result is very angle dependent. If only small incident angle reflections are taken into account, the image close to the well is best but imaging radius is very limited. Contributions from larger incident angles dominate the image further away from the well. The area close to the well is not illuminated in these cases. The blank zone is however obscured by energy smearing in from the sides due to the effect of limited lateral resolution. Figure 11 therefore indicates why depth migrated data should be interpreted angle range by angle range.

Note that synthetic PSDM results could have been generated by a "brute force" approach as well, i.e., by modelling raw 3D VSP data that are subsequently processed. However, ray-based simulation is much faster and more flexible and can be used in sensitivity workflows for a range of different boundary conditions to be tested. As this kind of simulation implies ideal processing, each result represents the best possible PSDM image and thus some upper limit of information to be expected for a given model and a given survey.

Concluding Remarks

Advanced ray-based approaches are ideally suited for survey planning and interpretation support and have evolved far beyond the means of conventional two-point ray-tracing. Ray based methods are more flexible and more efficient than FD modelling (note that none of the results shown in this article took more than 10 minutes of total processing time on a 20 node Linux cluster). In the remaining cases that would require FD modelling for valid reasons, ray-based methods are still supportive and complimentary.

References

Bear, G., Lu, C.-P., Lu, R., Willen, D., and Watson, I., 2000, The construction of subsurface illumination and amplitude maps via ray tracing, The Leading Edge, Vol. 19, 726-728.

Christian, P.J., Pringle, T., Zühlsdorff, L., Drottning, Å., Brown, G., and Webb, B., 2012, A survey design case history using complimentary raytracing and wavefield extrapolation techniques, 74th EAGE conference, Copenhagen, Extended Abstracts, Z016.

Drottning, Å., Branston, M., and Lecomte, I., 2009, Value of illumination consistent modeling in time-lapse seismic analysis, First Break, Vol. 27, 75-83.

Frazer, L.N., and Sen, M.K., 1985, Kirchhoff-Helmholtz reflection seismograms in a laterally inhomogeneous multi-layered elastic medium I. Theory, Geophysical Journal of the Royal Astronomical Society, Vol. 80, 121-147.

Gjøystdal, H., Iversen, E., Lecomte, I., Kaschwich, T., Drottning, Å., and Mispel, J, 2007, Improved applicability of raytracing in seismic acquisition, imaging and interpretation, Geophysics, Vol. 72, 261-271.

Houbiers, M., Arntsen, B., Mispel, J., Hager, E., Brown, G., and Hill, D., 2008, Full azimuth seismic modeling in the Norwegian Sea, 78th SEG conference, Las Vegas, Extended Abstracts, 2102-2106.

Ibrahim, A., 2005, 3D ray-trace modeling to assess the effects of overburden and acquisition geometry on illumination of pre-evaporite reservoirs in Karachaganak Field, Kazakhstan, The Leading Edge, Vol. 24, 940-944.

Laurain, R., Vinje, V., and Strand, C., 2004, Simulated migration amplitude for improving amplitude estimates in seismic illumination studies, The Leading Edge, Vol. 23, 240-245.

Lecomte, I., 2008, Resolution and illumination analyses in PSDM: A ray based approach, The Leading Edge, Vol. 27, 650-663.

Lou, M., Williamson, R., and Quinn, D., 2011, A methodology to estimate maximum offset and reflection imaging radius for 2D/3D VSP survey, EAGE Borehole Geophysics Workshop, Istanbul, Extended Abstracts, BG09.

Stork, C., 2012, Testing different 3D acquisition geometries for reducing back-scattered surface noise, 74th EAGE conference, Copenhagen, Extended Abstracts, X037.

Tygel, M., Schleicher, J., and Hubral, P., 1994, Kirchhoff-Helmholtz theory in modeling and migration, Journal of Seismic Exploration, Vol. 3, 203-214.

Vinje, V., Åstebøl, K., Iversen, E., and Gjøystdal, H., 1999, 3-D ray modeling by wavefront construction in open models, Geophysics, Vol. 64, 1912-1919.

Zühlsdorff, L., Gjøystdal, H., Branston, M., Drottning, Å., Bergfjord, E., and Rasmussen, T., 2010, An improved survey evaluation and design workflow, 72nd EAGE conference, Barcelona, Extended Abstracts, P294.